Bundle-sheath cells: are leaf "water valves" controlled by their H^+-ATPase: "open" by xylem acidification, "closed" by xylem alkalinization

One-sentence summary:

Bundle-sheath cells can control the leaf hydraulic conductance by proton-pump-regulated xylem sap pH

Yael Grunwald*[1], Noa Wigoda*[1,3], Nir Sade[1,2], Adi Yaaran[1], Tanmayee Torne[1], Sanbon Chaka Gosa[1], Nava Moran[1] and Menachem Moshelion[1].

[1] The R.H. Smith Institute of Plant Sciences and Genetics in Agriculture, The R.H. Smith Faculty of Agriculture, Food and Environment, The Hebrew University of Jerusalem, Rehovot, 76100 Israel

[2] School of Plant Sciences and Food Security, The George S. Wise Faculty of Life Sciences at Tel-Aviv University, Tel Aviv 6997801, Israel.

[3] *Present address*: Life Sciences Core Facilities department, Weizmann Institute of Science, Rehovot 76100 Israel

* Both authors contributed equally to this work.

Abstract

● The leaf vascular bundle sheath cells (BSCs) that tightly envelop the leaf veins, are a selective and dynamic barrier to xylem-sap water and solutes radially entering the mesophyll cells. Under normal conditions, xylem-sap pH of <6 is presumably important for driving and regulating the transmembranal solute transport. Having discovered recently a differentially high expression of a BSC proton pump, AHA2, we now test the hypothesis that it regulates this pH and leaf radial water fluxes.

● We monitored the xylem-sap pH using the ratiometric fluorescent probe FITC-dextran fed into veins of detached leaves of WT Arabidopsis, AHA mutants, and *aha2* mutants complemented with *AHA2* gene solely in BSCs. We tested an AHA inhibitor and stimulator, and different pH buffers. We monitored their impact on the xylem-sap pH, the whole leaf hydraulic conductance (K_{leaf}) and the water osmotic permeability of isolated BSCs protoplasts (P_f).

● Our results demonstrated AHA2 indispensability for xylem-sap acidification, necessary, in turn, for elevating P_f and K_{leaf}. Conversely, elevating xylem-sap pH to 7.5, reduced significantly both P_f and K_{leaf}.

● All these demonstrate a causative link between AHA2 activity in BSCs and leaf water influx. This positions the BSCs as a pH-controlled transpiration valve in series with the stomata.

Key words

AHA, AHA2, ABA, *Arabidopsis thaliana* (Thale cress), Barrier, Bundle sheath, drought, H^+-ATPase, Leaf hydraulic conductivity (K_{leaf}), Water valve , Xylem-sap pH.

Introduction

The majority (95%) of nutrients and water which enter the plant through the roots move upward in a bulk flow via xylem vessels all the way into the leaf veins (Taiz and Zeiger, 2014). On its way out of the leaf xylem and into the leaf photosynthetic tissue, the mesophyll, this transpiration stream crosses a layer of parenchymatous cells (bundle sheath cells, BSCs) which tightly enwrap the entire vasculature (Kinsman and Pyke, 1998). BSCs have been shown to act as a selective barrier between the vein and the mesophyll. In a banana leaf, for example, they impeded the transport of sodium (Shapira et al., 2009) and of boron (Shapira et al., 2013). The transport of boron was also impeded in the leaves of Thelungiella (Lamdan et al., 2012) and of Arabidopsis (Shatil-Cohen and Moshelion, 2012). Importantly, the BSCs act also as a barrier to the passage of water (Shatil-Cohen et al., 2011; Pantin et al., 2013). However, it is still not clear (Geilfus, 2017) whether and how the apoplastic (xylem) milieu modulates the "barrier behavior" of the bundle sheath, and in particular, whether this behavior depends on the xylem sap pH.

Some direct determinations of leaf xylem pH placed it at 6.3-6.7 in cotton leaves (Hartung et al., 1988), or at 5.3 in sunflower leaves (Jia and Davies, 2007) but most frequently, under normal growth conditions the leaf apoplast pH is around 5.5-6 (reviewed by Grignon and Sentenac, 1991; Geilfus, 2017). The leaf xylem sap pH can change in response to changes in external conditions experienced by the root. For example, the tomato leaf xylem sap alkalinized when roots were supplied with nitrate (Jia and Davies, 2007). Barley leaf sub-stomatal apoplast also alkalinized as a response to salts (KCl, NaCl, $NaNO_3$) added to the roots (Felle et al., 2005). Drying soil in tomato (Jia and Davies, 2007) and in *Vicia faba* (Karuppanapandian et al., 2017) or cold stress at the root level in barley (Felle et al., 2005) also caused alkalinization (measured, respectively in the tomato xylem sap, in the *V. faba* xylem sap and leaf apoplast, and in the barley sub-stomatal apoplast). Finally, alkalinization of the barley leaf sub-stomatal

apoplast was brought about also by applying ABA (considered not only a drought-stress hormone, but also shown to mediate cold stress (Huang et al., 2017)) both to barley roots and to detached leaves (Felle et al., 2005).

In turn, changes in the leaf xylem sap pH regulate physiological processes. Feeding high-pH solutions to detached leaves reduced stomatal conductance and transpiration both in *Commelina communis* and in tomato (Wilkinson and Davies, 1997; Wilkinson et al., 1998; Jia and Davies, 2007). As pH defines the dissociation state of weak acids, among them the major phytohormones abscisic acid (ABA) and indol acetic acid (IAA, auxin), changes in pH would affect both their distribution between the apoplast and the cellular compartments of the plant, and hence, their biological activities. For example, ABA accumulated in the alkalinizing xylem sap of a gradually pressure-dehydrated detached cotton leaf, which could be prevented by a pretreatment with an H^+-ATPase-activating fungal toxin, fusicoccin (Hartung et al., 1988). Leaf xylem alkalinization in *Vicia faba* as a result of gradually drying soil was followed by elevated ABA levels in the xylem (even if with a few days delay; Karuppanapandian et al., 2016).

Already widely-accepted is the crucial role of apoplastic protons in the proton-motive force governing transmembrane transport (Serrano, 1988, Haruta et al., 2012, Taiz and Zeiger, 2014), and, therefore, by extrapolation, the role of xylem sap pH – in *driving* the transport between the xylem and the surrounding BSCs (Shapira et al., 2009). Xylem pH may have also *regulatory* effects on the transport proteins in the BSCs membrane, including aquaporins. Surprisingly, however, even though aquaporins largely determine the osmotic membrane water permeability coefficient, P_f (see also Discussion), and while P_f, particularly the P_f of the BSCs, may well be important in determining the hydraulic conductance (K_{leaf}) of the entire leaf (Shatil-Cohen et al., 2011; Sade et al., 2014), the effect of *extra*cellular pH (or, rather, the lack thereof) has been mentioned only in passing in relation to the P_f of plasma membrane vesicles of *Beta vulgaris* storage root (Alleva et al., 2006) and was ignored in relation to tobacco aquaporins (NtPIP2;1 and NtPIP1) expressed in yeast (Fischer and Kaldenhoff, 2008). Thus, the effect of apoplastic

pH on P_f in other plant cells, and especially the effect of xylem sap pH on the BSCs P_f, is unknown. Furthermore, in spite of the importance of apoplast pH regulation of to the plant basic life processes (Haruta and Sussman, 2012), molecular evidence linking the leaf xylem sap regulation to a specific H^+-ATPase and to the ensuing physiological changes in the leaf is missing.

H^+-ATPases constitute a family of proton pumps driven by hydrolysis of ATP and are found in the plasma membrane of plants and fungi (Axelsen and Palmgren, 2001). 11 H^+-ATPases isoforms have been reported in Arabidopsis; among them, the AHA1 and AHA2 are by far the most abundantly expressed members of this family throughout plant life and tissues (Haruta et al., 2010). Both AHA2 (Wang et al., 2014) and AHA1 (Yamauchi et al., 2016) were found to take part in stomatal opening. In addition, the expression of a GUS reporter gene in Arabidopsis, under the *AHA2* promoter, revealed abundant expression specifically in roots and leaves, and especially in the vascular tissue (Fuglsang et al., 2007). Our transcriptome analysis of protoplasts isolated from Arabidopsis BSCs and mesophyll cells (MCs) showed that the BSCs express the *AHA2* gene abundantly and at a threefold higher level than the MCs, while the *AHA1* gene expression, though also abundant, was not different between these two cell types (the other 9 AHA isoforms were expressed at much lower leves in both cell types, Wigoda et al., 2017, as described generally for the whole plant, Haruta et al., 2010) .

Here we show how the BSCs act as a dynamic barrier for water flow between the xylem and mesophyll; we demonstrate a causative link between the activity of the BSCs AHA2 and the hydraulic conductance of the leaf and reveal that its underlying mechanism is the pH-controlled osmotic water permeability of the BSCs membranes.

Materials and Methods

Plant material

Plant types. We used WT (wild type) *Arabidopsis thaliana* plants ecotype Colombia, Col-0 (aka Col) and T-DNA insertion *AHA* mutants (Col): *AHA1* mutants: *aha1-6 (*SALK_ 016325), *aha1-7 (*SALK_ 065288) and *aha1-8* (SALK_ 118350), and *AHA2*

mutants; *aha2-4* (SALK_ 082786) and *aha2-5* (SALK_022010) obtained from the Arabidopsis Biological Resource Center (Ohio State University). The plants' genotypes were determined by PCR with allele-specific primers (supplemental Table S1) and then the single-gene mutants were confirmed for the near-absence of *AHA2 (or AHA1)* RNA using real time PCR (RT-PCR). For single-cell experiments, we used SCR:GFP (Col) Arabidopsis plants expressing GFP specifically in the BSCs ER generated in our lab and described in detail by Attia et al. (2018).

Plant Growth Conditions. All plants were grown in soil as described earlier (Shatil-Cohen et al., 2011). Plants were kept in a growth chamber under short-day conditions (10-h light) and a controlled temperature of 20–22°C, with 70% humidity. Light intensity at the plant height was 150-200 μmol m^{-2} sec^{-1} (an optimal level based on (Wu et al., 2009), achieved using either fluorescent lights (Osram cool white, T5 FH 35W/840 HE, Germany) or LED light (EnerLED 24V-5630, 24W/m, 3000K (50%)/6000K(50%)). The plants were irrigated twice a week.

Determination of xylem sap pH in detached leaves

Leaf perfusion. Leaves from 6-7 week old plants, approximately 2.5 cm long and 1 cm wide, were excised at the petiole base using a sharp blade and immediately dipped in "xylem perfusion solution" (XPS, see Solutions below), in 0.5 ml Eppendorf tubes for 30 minutes. Perfusion experiments using Safranin O (Sigma cat. #: S2255; 1% w/v in XPS) demonstrated that 30 minutes incubation sufficed for the whole leaf perfusion via the petiole by means of the transpiration stream (Fig. S1). All experiments were conducted between 1-4 hours from Lights On.

Sample preparation on the microscope stage. Immediately after the leaf xylem perfusion, the leaf was washed with that leaf's intended perfusate (the specific XPS to be tested) without a dye, laid on a microscope slide abaxial side up, and a drop of XPS (without the dye) was placed on top. Then, a thin layer of silicone high vacuum grease (Merck cat. #: 1.07921.0100) was applied around the leaf edge and a large coverslip (50

by 20 mm, larger than the leaf) was placed on the leaf and affixed to the slide beneath. The minor veins on the abaxial side were imaged via the coverslip.

Fluorescence microscopy was performed using an inverted microscope (Olympus-IX8 integrated within the Cell-R system, http://www.olympus-global.com), via an UPlanSApo 10*X*/0.40 (∞ /0.17/ FN26.5) objective. The leaf xylem pH was determined using the ratiometric (dual-excitation) membrane-impermeant fluorescent dye fluorescein isothiocyanate conjugated to 10 kD dextran (FITC-D;(Hoffmann and Kosegarten, 1995; Mühling et al., 1995; Pitann et al., 2009a; Pitann et al., 2009b) dissolved in the solution perfused into the detached leaf. Pairs of images were recorded at a single emission wavelength (520 nm) and the two excitation wavelengths (488 and 450 nm, applied approx. 200 ms apart; (Hoffmann and Kosegarten, 1995; Mühling et al., 1995)), using a 12-bit CCD camera, Orca-AG (Hamamatsu, http:// www.hamamatsu.com), and saved in a linear 16 bit tiff format for further processing.

In all fluorescence microscopy experiments, each treatment was performed on at least five leaves, each from a different plant, on three days (all together, five biological repetitions in three independent experiments per treatment), alternating randomly among different treatments. For each leaf, paired images of a minor vein were obtained from four to six different areas (four-six technical repetitions per a biological repeat). For background values, leaves were perfused with experimental solutions without the dye; one leaf was sampled per treatment or plant type on each day of an experiment (all together, at least three biological repetitions per treatment or plant type, a total of 20 leaves, with three technical repetitions per each biological repeat).

Image analysis. The images were processed with ImageJ (ver. 1.49V; http://rsbweb.nih.gov/ij/). A pixel by pixel ratio of the two images in each pair was calculated using the ImageJ 'Ratio-plus' plugin (Paulo J. Magalhães, 2004), after subtracting from each pixel's fluorescence the average background fluorescence at the corresponding excitation wavelength. Further analysis was performed on selected pixels, based on the image resulting from excitation at 488 nm: only pixels with fluorescence values below the camera saturation level (<4095) but at least 3 fold brighter than the

mean background value were selected (areas enclosed within yellow lines in the supplemental Fig. S2C).

pH calibration curve. An *in-vivo* pH calibration curve was constructed using XPS buffered to predefined pH values (5, 5.5,6, 6.5, 7 and 7.5; see Solutions below). This calibration curve served to convert the mean fluorescence ratio obtained from a minor vein segment to a pH value for each leaf (biological repeat). Occasionally, we verified the system stability using an *in-vitro* calibration curve derived from imaging drops of the calibration solutions placed on microscope slides rather than fed into leaf veins. Also, changing the composition of the buffers (MES and HEPES) in the XPS had no effect on the calibration curve.

Generation of SCR:AHA2-complemented plants

Vector construction: *AHA2* gene was cloned into pDONR™ 221 (Invitrogene) vector and the SCR promoter into pDONRP4P1r using Gateway® compatible by BP reactions, and later cloned into the pB7M24GW (Invitrogene) two fragment binary vector by LR reaction according to the manufacturer's instructions. The binary *SCR:AHA2* vector was transformed into Agrobacterium by electroporation; transformants were selected on LB plates containing 25 µg/mL gentamycin and 50 µg/mL spectinomycin.

aha2-4 and aha2-5 mutant lines transformation with *SCR:AHA2:* was performed using the floral dip method (Clough and Bent, 1998). Transformants were selected based on their BASTA resistance, grown on plates with MS (Murashige and Skoog, Duchefa cat# M222.0050) Basal medium + 1 % sucrose and 20 µg/ml BASTA (Glufosinate Ammonium, Sigma cat # 45520). DNA insertion was verified in selected lines by PCR targeting the junction of *AHA2* and the 35S terminator with forward primer about 1000bp from the 3' end of AHA2 and reverse primer on the 35S terminator (see primer list in supplemental Table S1).

AHA2 gene expression in the whole leaf by qRT-PCR

RNA extraction and quantitative real-time (qRT-) PCR. Total RNA was extracted from leaves using Tri-Reagent (Molecular Research Center, cat. #: TR 118) and treated with RNase-free DNase (Thermo Scientific™, cat. #: EN0525). Complementary DNA

(cDNA) was prepared using the EZ-First Strand cDNA synthesis kit (Biological Industries cat. #: 2080050) according to the manufacturer's instructions. qRT-PCR was performed using C1000 Thermal Cycler (Bio-Rad), in the presence of EvaGreen (BIO-RAD cat.# 172-5204) and PCR primers to amplify specific regions of the genome (Haruta et al., 2010; suppl. Table S1). The results were analyzed using Bio Rad CFX manager™ software. Dissociation curve analysis was performed at the end of each qRT-PCR reaction to validate the presence of a single reaction product and lack of primer dimerization. Expression levels of examined genes were normalized using two normalizing genes (AT5G12240 and AT2G07734, Wigoda et al., 2017).

Physiological characterization of the leaf (gas exchange and hydraulic conductance, K_{leaf})

Gas-exchange assays, i.e., g_s (stomatal conductance) and E (transpiration) were performed (as in Sade et al., 2014) using a Li-Cor 6400 portable gas-exchange system (LI-COR, USA https://www.licor.com/) equipped with a standard leaf cuvette with an aperture diameter of two cm^2, appropriate for Arabidopsis leaves using light intensity similar to the growth chamber conditions (illumination: 200 µmol m^{-2} s^{-1}; the amount of blue light was set to 10% of the photosynthetically active photon flux density, approximately 24 °C, the VPD: approximately 1.3 kPa, and [CO_2] surrounding the leaf: 400 µmol mol^{-1}). Readings were recorded at a steady state, 3-5 min after the leaf was clamped in the Li-Cor chamber.

Measuring the leaf water potential, Ψ_{leaf}. Immediately following the gas exchange measurement, the leaf was transferred to a pressure chamber (ARIMAD-3000; MRC Israel) equipped with a home-made silicon adaptor especially designed to fit Arabidopsis petioles into the chamber's O-ring. Ψ_{leaf} was determined as described earlier (Sade et al., 2014).

Determination of the leaf hydraulic conductance, K_{leaf}. K_{leaf} was calculated for each individual leaf as follows (Martre et al., 2000):

Eq. 1: $$K_{leaf} = E / (\Psi_{Leaf} - \Psi_{XPS}) \approx E / \Psi_{Leaf},$$

where E is the whole-leaf's transpiration, i.e., the water flux, and Ψ_{Leaf} is the leaf water potential and Ψ_{XPS} is the water potential of XPS (or of the XPS^{db}); as Ψ_{XPS} is nearly null, the leaf water potential value alone was used.

Sample preparation. In all K_{leaf} determinations, we followed our previous protocols (Shatil-Cohen et al., 2011; Sade et al., 2014; Sade et al., 2015) with a necessary adaptation in the present work (below) due to an approx. three-fold increase in the growth chamber light intensity (to 150-200 μmol m^{-2} sec^{-1}; (Wu et al., 2009)), which resulted in increased stomatal conductance and transpiration. Under these new conditions, the leaves excised for measurements (with petioles dipped in the different solutions) usually lost the turgor and collapsed within 20-30 minutes after Lights On (Suppl. Fig S3), making physiological measurements challenging. Therefore, to preserve their turgidity until measurements, the leaves (with their Eppendorf vials) were placed in "humidity boxes" i.e. sealed, 25 x 25 x 15 cm plastic transparent plastic boxes with damp tissue paper on the bottom (to provide ~80-90% humidity) and kept for 1-4 h in the growth room under the regular light and temperature conditions. 5 minutes prior to the measurements, the leaves were exposed to the ambient vapor pressure deficit (VPD) of 1.3-1.5 kPa outside the boxes, still under light. The measurements were conducted between 10:00 AM to 1:00 PM (1-4 hours after Lights On). The physiological relevance of this protocol was validated in preliminary assays (Suppl. Fig. S4), which agreed with the results of Scoffoni et al, 2018 for well hydrated Arabidopsis leaves.

For experiments of Suppl Figs. S5A, 5C, 5E, the leaves were excised in the evening preceding the measurements, in the light, shortly before the "Lights Off" transition, and placed in a humidity box which was placed, in turn, in another, lightproof box for the duration of the night. Measurements were conducted in the morning, between 10:00 AM and 13:00 PM, after 20 min of illumination in the growth chamber.

For experiments of Suppl. Figs. S5B, S5D, S5F, leaves were excised on the morning of the experiment, in the dark, about 10 min before the regular "Lights On" transition.

Protoplast isolation

Protoplasts were isolated from 6- to 8-week-old plants using the rapid method (Shatil-Cohen et al., 2014) using an isotonic solution in the extraction procces (pH 6, 600 mOsmol, see Solutions below).

Osmotic water permeability coefficient (P_f) measurements

P_f was determined as described by Shatil-Cohen et al. (2014), except here we used an inverted epifluorescent microscope (Nikon eclipse TS100) with a 20x/NA 0.40 objective (Nikon) and a CCD 12 bit camera Manta G-235B (https://www.alliedvision.com), and an image-processing software AcquireControl® v5.0.0 (https://www.alliedvision.com). We recorded the BSCs swelling in response to hypo-osmotic challenge (of 0.37 MPa) generated by changing the bath solutions from isotonic (600 mOsm) to a hypotonic one (450 mOsm, *ibid.*). The challenges were performed at pH 6 and at pH 7.5. The osmolarity of these solutions (variants of the XPS^{db}; see Solutions) was adjusted with the appropriate amounts of D-sorbitol and was verified within 1% of the target value using a vapour pressure osmometer (Wescor). P_f was determined from the initial rate of the cell volume increase using a numerical approach, in an offline curve-fitting procedure of the P_fFit program, as described in Shatil-Cohen et al., (2014) and detailed in Moshelion et al., (2004). We present here the values of the intital P_f (P_{f_i}) obtained by fitting model 5 (*ibid.*).

Solutions

FITC-D dye (Sigma cat. #: FD10S) was added from a 10 mM stock in water (kept aliquoted, protected from light, at -20 ^{o}C) to all the XPS solutions (except in the leaf-tissue-autofluorescence assays) to a final conc. of 100 µM.

XPS, basal Xylem Perfusion Solution: 1 mM KCl, 0.3 mM $CaCl_2$ and 20 mM D-sorbitol (Sigma cat# 8143). Upon preparation, when unbuffered, the pH of this solution was 5.6 - 5.8 and its osmolarity was approx. 23 mOsm/L.

Low-K^+ XPS: the same as XPS above.

High-K^+ XPS: XPS + 10 mM KNO_3 and D-sorbitol adjustment to approx. 23 mOsm/L. Upon preparation, when unbuffered, the pH of this solution was 5.6 -5.8.

XPS^{b} (pH calibration solutions): XPS buffered with 20 mM MES and HCl or NMG to pH 5, 5.5, or 6), or with 20 mM HEPES and NMG to pH 6.5, 7, or 7.5. Osmolarity of these solutions was adjusted with D-sorbitol to 23 mOsm/L.

XPS^{db}: High-K^+ XPS buffered with 10 mM MES and 10 mM HEPES and adjusted to pH 4.8, 6 or 7.5 with HCl or N-Methyl D-glucamine (NMG). These solutions were adjusted with D-sorbitol to a final osmolarity of 40 mOsm/L.

AXS: 3 mM KNO_3, 1 mM $Ca(NO_3)2$, 1 mM $MgSO_4$, 3 mM CaCl2, 0.25 mM NaH_2PO_4, 90 µM EDFC and a micro-nutrient mix of 0.0025 µM $CuSO_4$, 0.0025 µM H_2MoO_4, 0.01 µM $MnSO_4$, 0.25 µM KCl, 0.125 µM H_3BO_3, 0.01 µM $ZnSO_4$; 21 mosmol; pH of the unbuffered solution was 5.8.

Solutions for leaf physiological characterization: Non-buffered High-K^+ XPS (as above) was used for Figure 4A (and Suppl. Figs. S7A,S7C, S7E). AXS was used for fig 4B. XPS^{db} was used for Fig. 4C (and Suppl. Figs. S7B, S7D, S7F).

Solutions for P_f determination: <u>pH 6 solutions</u> : XPS^{db} adjusted to pH 6 by NMG, and adjusted with D-sorbitol to either 450 mOsmol (hypotonic) or 600 mOsmol (isotonic); <u>pH 7.5 solutions</u>: XPS^{db} adjusted to pH 7.5 by NMG, and adjusted with D-sorbitol to either 450 mOsmol (hypotonic) or 600 mOsmol (isotonic).

Solution for protoplasts isolation: pH 6 isotonic solution as for P_f determination.

Statistics

The Student's unpaired two-tailed t-test was used for comparison of two means, which were considered to be significantly different at $P < 0.05$. For comparisons of three or more population means we used ANOVA, all-pairs Tuckey HSD (JMP® Pro 13), wherein different letters represent statistical differences at $P<0.05$. Images which yielded extreme ratio values which were more than 2.5 SD away from the mean were discarded.

Results

The effect of pharmacological agents – a pump stimulator and an inhibitor – on xylem pH

We used the fluorescence of FITC-dextran (10 kDa) perfused via petioles into detached WT Arabidopsis leaves to monitor the pH within the leaf minor veins (Materials and methods, Suppl. Figs S1-S2). When 10 µM fusicoccin (a fungal stimulator of P-type proton pumps, Serrano, 1988) was fed into the xylem, we observed a sharp decrease in xylem sap pH of about two pH units compared with leaves in control conditions (Figs. 1Ai, 1Aii, 1B) approximately 30 minutes after addition of fusicoccin. ETOH, the fusicoccin solvent, by itself, had no impact on xylem pH (Suppl. Fig. S6).

Further, WT leaves treated with 1 mM of vanadate (a commonly used P-type H^+-pump inhibitor (reviewed by Palmgren, 2001), in a high-K^+ solution (10 mM KNO_3), resulted in xylem sap alkalization of about one pH unit within 30-40 min (Figs. 1Aiii, 1Aiv, 1C). Interestingly, neither a similar exposure to vanadate in the low-K^+ solution (XPS without added KNO_3, suppl. Fig.S4A), nor the high-K^+ solution by itself (Suppl. Fig. S7B) had any effect on the xylem sap pH.

AHA2 acidifies the xylem pH

In an attempt to resolve between the relative contributions of the two abundant H^+-ATPAses of the BSCs, AHA1 and AHA2 (Wigoda et al., 2017), to the acidification of the xylem pH, we compared the xylem sap pH of WT plants to that in T-DNA-insertion

mutants of either pump. We used two independent mutant lines with a homozygous loss of function of the *AHA2* gene (*aha2-4* and *aha2-5*) and three such lines with mutated *AHA1* (*aha1-6, aha1-7, aha1-8*). The xylem sap pH of both *AHA2* mutants, *aha2-4* and *aha2-5,* was consistently higher, by 0.5-1 pH units, compared to the WT plants (Fig. 2A). In contrast, there was no significant difference between the xylem sap pH in WT vs. the three lines of AHA1 mutants (Suppl. Fig. S8).

To further test the ability of AHA2 to acidify the xylem sap pH, we complemented the *AHA2* deficient plants (the *aha2-4* mutant), with the *AHA2* gene directed specifically to the BSCs (under the BSCs-specific promotor Scarecrow, SCR; Wysocka-Diller et al., 2000). Using qRT-PCR on whole leaves of mature transgenic plants, we confirmed *AHA2* absence in the *aha2-4* mutant (Fig. 3A, as in Haruta et al., 2010), and demonstrated successful complementation in two lines (T55 and T56). The transcript level of *AHA2* in these lines was even higher than in the WT (Fig. 3A). While the xylem sap pH in the *AHA2*- mutant, *aha2-4*, was significantly more alkaline than in WT plants (repeating the results of Fig. 2A above), upon the complementation of the *aha2-4* mutant with the BSC-directed *AHA2*, the xylem sap pH in both lines became no higher than WT (Fig 3B). The level of *AHA1* transcript in the whole leaf was not affected by the genetic manipulations of AHA2, neither by *AHA2* mutation (as in Haruta et al., 2010), nor by the BSC-specific mutant complementation with *AHA2* (Fig. 6).

Elevating pH lowers the leaf hydraulic conductance, K_{leaf}

To examine the impact of AHA2 on the water economy of the whole leaf we determined the leaf water potential (Ψ_{leaf}) and its transpiration (E), and from these two we calculated the leaf hydraulic conductance (K_{leaf}, Eq. 1 in Materials and methods). We compared the K_{leaf} in detached leaves of WT and of the *aha2-4* and *aha2-5* mutants fed with unbuffered XPS. Notably, the K_{leaf} of the mutants was appreciably lower than that of WT leaves, about 50 % of WT in *aha2-4* and about 30 % in *aha2-5* (Fig. 4A), although all three leaf types transpired at a similar rate (Suppl. Figs. S5A and S5E).

We then compared the K_{leaf} of WT, and aha2-4 complemented with the BSCs-directed *AHA2* (i.e., *AHA2* under the Scarecrow promoter; line T56, which presented the lowest xylem pH of all genetic lines; Fig. 3B). K_{leaf} of the aha2-4 was again about 50% lower than of the WT but K_{leaf} of the AHA2-complemened T56 line became no different from K_{leaf} of the WT (Fig. 4B). Furthermore, K_{leaf} of WT leaves perfused with XPS^{db} buffered at pH 7.5 was lower by over 50% compared to WT leaves perfused with XPS^{db} buffered at pH 6 (Fig. 4C), while K_{leaf} of leaves perfused with the more acidic pH 4.8 was not changed compared to the "normal" pH 6 (Fig. 4C). Notably, under neither of these three pH treatments was there a difference in the transpiration rate (Suppl. Figs. S5B and S5F).

Alkaline pH lowers the osmotic water permeability coefficient of BSCs protoplast membrane, P_f

In order to test the hypothesis that the pH-dependent reduction in K_{leaf} is due to a reduction in the water permeability of the BSCs membranes, we measured the osmotic water permeability coefficient, P_f, of BSC under two pH treatments, using GFP labeled BSCs, from SCR:GFP plants. The mean initial P_f (see Materials and methods) of BSCs treated with pH 6 was ~8.5 fold higher than that of BSCs treated with pH 7.5. (5.39 ± 1 µm sec^{-1} and 0.63 ± 0.2 µm sec^{-1}, respectively, Fig. 5).

Discussion

The AHA2 of the BSCs is indispensable for the leaf xylem sap acidification

H^+-ATPases are well known regulators of the apoplastic pH which has a key role in cell ion homeostasis. Here we demonstrate specifically that the H^+-ATPase AHA2 which resides in the BSCs plasma membrane, exerts a dominant role in the acidification of the xylem sap in leaves. This conclusion is based on four different complementing approaches used in our study.

(1) *In-vivo measurement of xylem pH*. In using the membrane-impermeable FITC-dextran fed to the Arabidopsis leaf via a petiole, we relied on earlier demonstrations (a)

of the tight isolation of the vascular system due to the bundle sheath (Kinsman and Pyke, 1998; Shatil-Cohen et al., 2011; Shatil-Cohen and Moshelion, 2012; Sade et al., 2014) and (b) the previous uses of this ratiometric pH probe in planta (Materials and Methods). We were thus satisfied that the FITC-D probe remained confined within the BSC-lined xylem apoplast of the minor veins and reported reliably on its pH (Fig. 1A).

(2) *The use of classical pharmacological agents*. An H^+-ATPase specific stimulator (fusicoccin) and inhibitor (vanadate), fed directly to the leaf xylem, established that pH acidification of the leaf xylem sap involves P-type proton pump(s) (AHAs), which extrude protons – most likely, from the BSCs – into the xylem lumen. Notably, in our experiments, vanadate increased the xylem sap pH only when it was administered in high-K^+ XPS, while vanadate in low-K^+ XPS did not cause any detectable pH change. We explain this requirement for 10 mM KNO_3 to show vanadate inhibition of the H^+-pump, as resulting from an increased concentration of substrate (the added K^+ and NO_3^- ions) which can participate in secondary H^+-co-transport into the BSCs, thereby dissipating the protons from the xylem lumen. This conforms with the aforementioned general notion that the pH of an apoplastic compartment reflects, among others, a balance in bi-directional proton movements (Serrano, 1988). That proton-coupled K^+ transmembrane co-transport plays a particularly important role in the BSCs is suggested by the 10% higher expression in BSCs (relative to mesophyll cells) of two K^+ uptake permeases, AtKT2 and AtKUP11 (likely to be H^+-coupled (Wigoda et al., 2017) and references therein).

(3) *Genetic manipulation.* A comparison of mutant lines to the wild type revealed that while the pH of the xylem sap in the *aha1* mutant lines was no different than in WT (Fig. S5), the pH of the xylem sap in both AHA2 mutant lines, a*ha2-4* and *aha2-5* was consistently higher than in WT (Fig. 2).

(4) *Genetic manipulation – complementation.* The xylem sap pH was restored to WT-like levels in two lines resulting from *aha2-4* complementation with the *AHA2* gene directed specifically into the BSCs, using the specific promotor SCR.

Notwithstanding the above findings, we have not ruled out completely a potential contribution of AHA1 to the xylem pH. While the quite abundant AHA1 transcript level (Wigoda et al., 2017) remained unaffected by genetic manipulations of AHA2 (Suppl. Fig. S3), contrary to what might be expected had they been linked by a mutual feedback because of shared responsibility for the same function, a compensatory feedback may have occurred at the level of protein activity. Moreover, since the double aha1-aha2 mutant is embryonic-lethal (Haruta et al., 2010), the potential contributions of AHA1 (and of other AHAs, with much lower transcript levels) to xylem sap pH was not assessed more critically.

Extracellular pH regulation of the membrane osmotic water permeability

Earlier work established that low *cytosolic* pH reduces the membrane osmotic water permeability coefficient, P_f, by inhibiting aquaporin gating (Gerbeau et al., 2002; Tournaire-Roux et al., 2003; Alleva et al., 2006; Fischer and Kaldenhoff, 2008; Leitão et al., 2012; Frick et al., 2013; Yaneff et al., 2016). This phenomenon is especially relevant to roots under stress conditions such as flooding or drought, where a change in the water hydraulic permeability of the roots is considered to be part of the plant stress defense mechanism.

External pH seemed not to affect the membrane hydraulic permeability of intact cells (Lp) of Nitella, Chara and maize, except a slight inhibition at pH around 4.5 in Nitella and in one variety of maize (Tyerman et al., 2002 and references therein).

P_f sensitivity to pH has been also found in several mammalian cell types, be it cytosolic pH (Kaptan et al., 2015; Gotfryd et al., 2018), or extracellular pH (Mosca et al., 2018). Here we demonstrate, for the first time in an intact plant protoplast, the BSC, a reduction in P_f by *external* (xylem sap) alkalinization. This pH sensitivity differs from the *lack* of external pH effect on the right-side-out plasma membrane vesicles of *Beta vulgaris* root (Alleva et al., 2006). However, this difference is not surprising, in view of the differences between root and shoot, for example, in their opposite responses to drought:

acidification in the root xylem sap and alkalinization in the shoot xylem sap (Karuppanapandian et al., 2017).

"Macroscopic" membrane P_f changes and, moreover, whole-organ K_{leaf} changes have been tied to changes in aquaporin activity. For example, Shatil-Cohen et al. (2011), reduced both P_f and K_{leaf} by a common aquaporin blocker $HgCl_2$. Also, Prado et al. demonstrated that three aquaporins expressed in veins, and in particular, PIP2;1, contributed to darkness-enhanced hydraulic water conductance of the Arabidopsis leaves rosette (Prado et al., 2013). Additionally, BSCs-directed knockdown of aquaporins (using artificial microRNAs under the SCR promoter) decreased the K_{leaf} of a detached Arabidopsis leaf and, separately, BSCs P_f (Sade et al., 2014). Therefore, it is interesting to compare the external pH effect we observed on the P_f of BSCs to the effects of external pH on aquporins. For example, an external acidification (from pH 7.4 to pH 5), perceived via external tyrosine and histidine, *decreased* the permeability to water and glycerol of the human aquaglyceroporin, AQP7, with a half-inhibition at about pH 6 (Mosca et al., 2018); in contrast, the fungal aquaporin RdAQP1 activity (when expressed in Arabidopsis protoplasts) was enhanced at acidic external pH and inhibited at alkaline external pH (Turgeman et al., 2016).

Like RdAQP1, at least several Arabidopsis aquaporins have histidines (pka = 6.8) and/or cysteins (pKa=8.5) in their apoplast-facing loops, and also plenty of tyrosines (pKa=10). For example (even excluding tyrosines, because of their high pKa), based on uniprot membrane topology (www.uniprot.org/), PIP2;1 has exterior-facing Cys75 and His248; PIP2;2, has exterior-facing Cys73; His246; PIP2;3: Cys73, His148,-246, etc. Future work will clarify whether the P_f reduction in BSCs and the reduction of K_{leaf} in detached Arabidopsis leaves (see also further discussion of K_{leaf} and P_f relationship below) is also mediated by aquaporins and their external histidines/cysteins.

AHA2 role in the regulation of the whole leaf water balance

The notion that AHA pumps, in general, power secondary H^+-cotransport across cell membranes facing the apoplast is decades old (Serrano, 1988; Sze et al., 1999; Palmgren,

2001). The plant plasma membrane H^+-ATPase has since been recognized as essential for plant growth (reviewed by Falhof et al., 2016). The practically sole "celebrated product" of its action to date is the proton motive force (PMF) – a gradient of protons concentration without- or in combination with an electrical gradient – which drives the movement of solutes across cellular membranes. In only a few cases has a *specific* physiological role been assigned to the plasma membrane H^+-ATPase – mainly in stomatal physiology and in roots (reviewed by Falhof et al., 2016).

Here we show another, novel aspect of transport activity *regulated* (rather than *driven*) by AHA2 – that of water fluxes from the xylem into the leaf and across the bundle sheath layer – evident as the leaf hydraulic conductance, K_{leaf}. When pH is manipulated directly by buffers in the range of pH 6 to 7.5 we demonstrate a causative inverse correlation between the xylem sap pH and the resulting K_{leaf} (Figs. 4C). We observe a similar trend when pH is altered genetically: abolishing AHA2 activity (in *aha2* mutants), raises the xylem pH relative to WT and reduces K_{leaf} (Figs. 3B, 6).

Since an optimum function usually indicates at least two different underlying processes, we interpret the leveling off of K_{leaf} in the more acidic range of the xylem perfusion solution (pH 4.8 in Figs. 4C, pH ≤pH 5.1 in Fig. 6), showing perhaps even a hint of a decline relative to K_{leaf} values at higher pH values, as separable from the mechanism underlying the decline of Kleaf at *increasing* pH values, which we link to the cessation of (at least) the AHA2 activity.

The above considerations of AHA2 role invite a speculation with regard to the role of the plant stress hormone, abscisic acid (ABA) in regulating K_{leaf}. In an earlier work, Shatil-Cohen et al. (Shatil-Cohen et al., 2011) localized K_{leaf} to the BSCs layer by showing that K_{leaf} decreased when the BSCs were brought into direct contact with ABA fed to the detached leaf, and not when ABA was smeared on the leaf surface. Our current work outlines a mechanism for this phenomenon: stress-induced xylem alkalinization (already reported by others (Jia and Davies, 2007; Wang et al., 2012; Korovetska et al., 2014), likely due to ABA inhibition of the BSCs AHA2, similar to the H^+-ATPase inhibition

seen in guard cells (Goh et al., 1996; Schroeder et al., 2001; Zhang et al., 2004), reduces the water permeability of the BSCs membranes. Consequently, the water permeability of the entire bundle sheath layer declines, demonstrating that under stress conditions it is an active hydraulic barrier (Shatil-Cohen et al., 2011, Pantin et al., 2013). Here we show directly, using individual isolated BSCs, that P_f, the measure of the rate of water passage via the BSCs membranes, declines with external medium alkalinization (Fig. 5). Such a pH rise could mediate the effect of ABA on BSCs in the detached leaf.

In the whole plant, leaf water balance (leaf relative water content or leaf water potential) is determined by the ratio between the movement of water (liquid) from the xylem into the leaf and the movement of water (gas) out of the leaf via guard cells. This ratio depends, in turn, on the ratio between K_{leaf} and the stomatal conductance (Levin et al., 2007; Ache et al., 2010; Nardini et al., 2011; Shatil-Cohen et al., 2011). Decline in soil moisture usually acoompanies an increased drive (VPD) for transpiration (Oishi et al., 2010). Therefore, maintaining a sufficient supply of water to the leaves is challenging because the cohesion-tension mechanism allowing water flux during transpiration places the xylem under tension, making it vulnerable to cavitation-induced embolisms (Zimmermann, 1983). The observed variations in transpiration rate of whole plants have been proposed to reflect internal adjustments protecting the plant against such challenges of changing ambient conditions (Wallach et al., 2010; Scoffoni et al., 2017; Scoffoni et al., 1918). We propose here that the dynamic adjustments in water flux through the transpiring leaf are due to the dynamic changes of BSCs' P_f in response to changes of xylem sap pH and the consequent changes in K_{leaf}. In a transpiring plant, K_{leaf} decreases as a consequence of xylem alkalinization in the shoot, which signals a decline of soil moisture. The K_{leaf} decrease is what prevents further water escape from the xylem and decreases the water tension in the xylem, diminishing the danger of cavitation and embolism.

The results of this study broaden our basic understanding of how a leaf controls its water influx. Our results also support the notion that xylem sap alkalinization mediates the

decline in plant shoot nutrient uptake due to abiotic stress. Here we focus specifically on the stress-induced cessation of activity of AHA2 in the BSCs, where we found the AHA2 instrumental in generating the low pH in the leaf xylem sap. The consequence of this decline of AHA2 activity and xylem sap alkalinization, is a decline in the PMF. Since AHA2 – via the PMF – powers the secondary, proton-coupled export and import of solutes across the BSCs membranes, not only does it regulate plant nutrition, but, very likely also drives the extrusion of toxic compounds from the xylem-lining cells into the xylem, hence governing also the plant toxicity tolerance. These hypotheses await future experimentation.

In conclusion, our finding that AHA2 plays a major role in regulating K_{leaf} via xylem sap pH provides a molecular basis for understanding a novel aspect, other than just PMF, of the control that the xylem sap pH can exert in the leaf. This control, in combination with effects of PMF, is likely to underlie the plant's key physiological activities. These results provide a new focus for exploration and understanding the role of the involvement of BSCs in determining the xylem sap composition, and, in particular, their role as a transpiration-controlling valve in series with the stomata. As the rapid growth rate and high yields of crop plants are positively correlated with enhanced transpiration and K_{leaf}, BSCs are likely to become a key target tissue for the development of a new generation of manipulations for plant adaptation to environmental challenges.

Acknowledgments

We thank Ms. Dvorah Weisman of the Hebrew University of Jerusalem for help with image analysis and Dr. Shifra Ben-Dor of the Weizmann Institute of Science for comments on the manuscript.

This research was supported by the Israel Science Foundations, ISF (grants No.1312/12, and 1842/13 to NM, grant No. 878/16 to MM and a grant No. 12-01-0007 from the Israeli Chief Scientist, Ministry of Agriculture & Rural Development to MM and NM).

Author Contributions

Author contributions:

N. Wigoda and Y. Grunwald planned performed and analyzed the experiments, and wrote the paper. A. Yaaran and T. Torne participated in generating the complemented plant lines, and A. Yaaran and S. Gosa participated in the leaf hydraulics determinations. N. Sade participated in the genotyping of the mutant AHA lines. M. Moshelion and N. Moran conceived the experiments, guided the students and wrote the paper.

Competing interests

All authors declare they have no competing interests.

Supplementary Materials

Figure S1. Perfusion of detached leaves via petioles

Figure S2. Image analysis details

Figure S3. The reversibility of wilting of detached Arabidopsis leaves.

Figure S4. Physiological responsiveness of leaves during transition from ‘humidity boxes’ to open air.

Figure S5. Knockout of AHA2 or alkaline xylem sap pH decrease K_{leaf} in detached leaves.

Figure S6. Fusicoccin (and not its solvent EtOH by itself) lowered the leaf xylem sap pH

Figure S7. Neither vanadate in the *low-K^+* XPS nor the high-K^+ XPS *without* vanadate affect the xylem sap pH in WT Arabidopsis

Figure S8. Knockout of AHA1 does not increase xylem sap pH in minor leaf veins of Arabidopsis leaf.

Figure S9. Expression levels of *AHA1* in leaves of WT, *aha2-4* and of two independent bundle-sheath-specific AHA2-complimented lines (T55, T56)

Table S1. List of primers used for genotyping (PCR) and expression quantification (RT-PCR) of AHA1 and AHA2 in mutants and transformed plants.

References and Notes

Ache P, Bauer H, Kollist H, Al-Rasheid KAS, Lautner S, Hartung W, Hedrich R (2010) Stomatal action directly feeds back on leaf turgor: New insights into the regulation of the plant water status from non-invasive pressure probe measurements. Plant J **62**: 1072–1082

Alleva K, Niemietz CM, Sutka M, Maurel C, Parisi M, Tyerman SD, Amodeo G (2006) Plasma membrane of Beta vulgaris storage root shows high water channel activity regulated by cytoplasmic pH and a dual range of calcium concentrations. J Exp Bot **57**: 609–621

Attia Z, Dalal A, Moshelion M (2018) Vascular bundle sheath and mesophyll regulation of leaf water balance in response to chitin. bioRxiv. doi: 10.1101/337709

Axelsen KB, Palmgren MG (2001) Inventory of the superfamily of P-type ion pumps in Arabidopsis. Plant Physiol **126**: 696–706

Clough SJ, Bent AF (1998) Floral dip: A simplified method for Agrobacterium-

mediated transformation of Arabidopsis thaliana. Plant J **16**: 735–743

Falhof J, Pedersen JT, Fuglsang AT, Palmgren M (2016) Plasma membrane H+-ATPase regulation in the center of plant physiology. Mol Plant **9**: 323–337

Felle HH, Herrmann A, Hückelhoven R, Kogel KH (2005) Root-to-shoot signalling: Apoplastic alkalinization, a general stress response and defence factor in barley (Hordeum vulgare). Protoplasma **227**: 17–24

Fischer M, Kaldenhoff R (2008) On the pH regulation of plant aquaporins. J Biol Chem **283**: 33889–33892

Frick A, Järvå M, Törnroth-Horsefield S (2013) Structural basis for pH gating of plant aquaporins. FEBS Lett **587**: 989–993

Fuglsang AT, Guo Y, Cuin T a, Qiu Q, Song C, Kristiansen K a, Bych K, Schulz A, Shabala S, Schumaker KS, et al (2007) Arabidopsis protein kinase PKS5 inhibits the plasma membrane H+ -ATPase by preventing interaction with 14-3-3 protein. Plant Cell **19**: 1617–34

Geilfus CM (2017) The pH of the apoplast: dynamic factor with functional impact under stress. Mol Plant **10**: 1371–1386

Gerbeau P, Amodeo G, Henzler T, Santoni V, Ripoche P, Maurel C (2002) The water permeability of *Arabidopsis* plasma membrane is regulated by divalent cations and pH. Plant J **30**: 71–81

Goh CH, Kinoshita T, Oku T, Shimazaki K (1996) Inhibition of blue light-dependent H+ pumping by abscisic acid in Vicia guard-cell protoplasts. Plant Physiol **111**: 433–440

Gotfryd K, Mósca AF, Missel JW, Truelsen SF, Wang K, Spulber M, Krabbe S, Hélix-Nielsen C, Laforenza U, Soveral G, et al (2018) Human adipose glycerol flux is regulated by a pH gate in AQP10. Nat Commun **9**: 4749

Grignon C, Sentenac H (1991) pH and ionic conditions in the apoplast. Annu Rev Plant Physiol Plant Mol Biol **42**: 104–121

Hartung W, Radin JW, Hendrix DL (1988) Abscisic acid movement into the

apoplastic solution of water-stressed cotton leaves: role of apoplastic pH. Plant Physiol **86**: 908–913

Haruta M, Burch HL, Nelson RB, Barrett-Wilt G, Kline KG, Mohsin SB, Young JC, Otegui MS, Sussman MR (2010) Molecular characterization of mutant Arabidopsis plants with reduced plasma membrane proton pump activity. J Biol Chem **285**: 17918–29

Haruta M, Sussman MR (2012) The effect of a genetically reduced plasma membrane protonmotive force on vegetative growth of Arabidopsis. Plant Physiol **158**: 1158–71

Hoffmann B, Kosegarten H (1995) FITC-dextran for measuring apoplast pH and apoplastic pH gradients between various cell types in sunflower leaves. Physiol Plant **95**: 327–335

Huang X, Shi H, Hu Z, Liu A, Amombo E, Chen L, Fu J (2017) ABA Is Involved in Regulation of Cold Stress Response in Bermudagrass. Front Plant Sci **8**: 1613

Jia W, Davies WJ (2007) Modification of leaf apoplastic pH in relation to stomatal sensitivity to root-sourced abscisic acid signals. Plant Physiol **143**: 68–77

Kaptan S, Assentoft M, Schneider HP, Fenton RA, Deitmer JW, MacAulay N, De Groot BL (2015) H95 Is a pH-Dependent Gate in Aquaporin 4. Structure **23**: 2309–2318

Karuppanapandian T, Geilfus C-M, Mühling K-H, Novák O, Gloser V (2017) Early changes of the pH of the apoplast are different in leaves, stem and roots of Vicia faba L. under declining water availability. Plant Sci **255**: 51–58

Kinsman EA, Pyke KA (1998) Bundle sheath cells and cell-specific plastid development in Arabidopsis leaves. Development **125**: 1815–1822

Korovetska H, Novák O, Jůza O, Gloser V (2014) Signalling mechanisms involved in the response of two varieties of Humulus lupulus L. to soil drying: I. changes in xylem sap pH and the concentrations of abscisic acid and anions.

Plant Soil **380**: 375–387

Lamdan NL, Attia Z, Moran N, Moshelion M (2012) The Arabidopsis-related halophyte Thellungiella halophila: boron tolerance via boron complexation with metabolites? Plant Cell Environ **35**: 735–46

Leitão L, Prista C, Moura TF, Loureiro-Dias MC, Soveral G (2012) Grapevine aquaporins: Gating of a tonoplast intrinsic protein (TIP2;1) by cytosolic pH. PLoS One. doi: 10.1371/journal.pone.0033219

Levin M, Lemcoff JH, Cohen S, Kapulnik Y (2007) Low air humidity increases leaf-specific hydraulic conductance of Arabidopsis thaliana (L.) Heynh (Brassicaceae). J Exp Bot **58**: 3711–3718

Martre P, Durand JL, Cochard H (2000) Changes in axial hydraulic conductivity along elongating leaf blades in relation to xylem maturation in tall fescue. New Phytol **146**: 235–247

Mósca A, de Almeida A, Wragg D, Martins A, Sabir F, Leoni S, Moura T, Prista C, Casini A, Soveral G (2018) Molecular Basis of Aquaporin-7 Permeability Regulation by pH. Cells **7**: 207

Moshelion M, Moran N, Chaumont F (2004) Dynamic changes in the osmotic water permeability of protoplast plasma membrane. Plant Physiol **135**: 2301–2317

Mühling KH, Plieth C, Hansen U, Sattelmacher B (1995) Apoplastic pH of intact leaves of Vicia faba as influenced by light. J Exp Bot **46**: 377–382

Nardini A, Salleo S, Jansen S (2011) More than just a vulnerable pipeline: xylem physiology in the light of ion-mediated regulation of plant water transport. J Exp Bot **62**: 4701–18

Oishi AC, Oren R, Novick KA, Palmroth S, Katul GG (2010) Interannual Invariability of Forest Evapotranspiration and Its Consequence to Water Flow Downstream. Ecosystems **13**: 421–436

Palmgren MG (2001) Plant plasma membrane H+ -ATPases□: Powerhouse for nutrient uptake. Annu Rev Plant Physiol Plant Mol Biol **52**: 817–45

Pantin F, Monnet F, Jannaud D, Costa JM, Renaud J, Muller B, Simonneau T, Genty B (2013) The dual effect of abscisic acid on stomata. New Phytol **197**: 65–72

Paulo J. Magalhães (2004) Ratio Plus (ImageJ) https://imagej.nih.gov/ij/plugins/ratio-plus.html.

Pitann B, Kranz T, Mühling KH (2009a) The apoplastic pH and its significance in adaptation to salinity in maize (Zea mays L.): Comparison of fluorescence microscopy and pH-sensitive microelectrodes. Plant Sci **176**: 497–504

Pitann B, Schubert S, Mühling KH (2009b) Decline in leaf growth under salt stress is due to an inhibition of H^+-pumping activity and increase in apoplastic pH of maize leaves. J Plant Nutr Soil Sci **172**: 535–543

Prado K, Boursiac Y, Tournaire-Roux C, Monneuse J-M, Postaire O, Da Ines O, Schaffner AR, Hem S, Santoni V, Maurel C (2013) Regulation of Arabidopsis Leaf Hydraulics Involves Light-Dependent Phosphorylation of Aquaporins in Veins. Plant Cell **25**: 1029–1039

Sade N, Shatil-Cohen A, Attia Z, Maurel C, Boursiac Y, Kelly G, Granot D, Yaaran A, Lerner S, Moshelion M (2014) The Role of Plasma Membrane Aquaporins in Regulating the Bundle Sheath-Mesophyll Continuum and Leaf Hydraulics. PLANT Physiol **166**: 1609–1620

Sade N, Shatil-Cohen A, Moshelion M (2015) Bundle-sheath aquaporins play a role in controlling Arabidopsis leaf hydraulic conductivity. Plant Signal Behav **10**: e1017177

Schroeder JI, Allen GJ, Hugouvieux V, Kwak JM, Waner D (2001) Guard cell signal transduction. Annu Rev Plant Physiol Plant Mol Biol **52**: 627–658

Scoffoni C, Albuquerque C, Brodersen CR, Townes S V., John GP, Bartlett MK, Buckley TN, McElrone AJ, Sack L (2017) Outside-Xylem Vulnerability, Not Xylem Embolism, Controls Leaf Hydraulic Decline during Dehydration. Plant Physiol **173**: 1197–1210

Serrano R (1988) Structure and function of proton translocafing ATPase in

plasma membranes of plants and fungi. Biochim Biophys Acta - Rev Biomembr **947**: 1–28

Shapira O, Israeli Y, Shani U, Schwartz A (2013) Salt stress aggravates boron toxicity symptoms in banana leaves by impairing guttation. Plant, Cell Environ **36**: 275–287

Shapira O, Khadka S, Israeli Y, Shani U, Schwartz A (2009) Functional anatomy controls ion distribution in banana leaves: Significance of Na + seclusion at the leaf margins. Plant, Cell Environ **32**: 476–485

Shatil-Cohen A, Attia Z, Moshelion M (2011) Bundle-sheath cell regulation of xylem-mesophyll water transport via aquaporins under drought stress: a target of xylem-borne ABA? Plant J **67**: 72–80

Shatil-Cohen A, Moshelion M (2012) Smart pipes: the bundle sheath role as xylem-mesophyll barrier. Plant Signal Behav **7**: 1088–91

Shatil-Cohen A, Sibony H, Draye X, Chaumont F, Moran N, Moshelion M (2014) Measuring the osmotic water permeability coefficient (Pf) of spherical cells: isolated plant protoplasts as an example. J Vis Exp e51652

Sze H, Li X, Palmgren M (1999) Energization of plant cell membranes by H+-pumping ATPases. Regulation and biosynthesis. Plant Cell **11**: 677–690

Taiz L, Zeiger E (2014) Plant Physiology and Development. doi: 10.3119/0035-4902-117.971.397

Tournaire-Roux C, Sutka M, Javot H, Gout E, Gerbeau P, Luu DT, Bligny R, Maurel C (2003) Cytosolic pH regulates root water transport during anoxic stress through gating of aquaporins. Nature **425**: 393–397

Turgeman T, Shatil-Cohen A, Moshelion M, Teper-Bamnolker P, Skory CD, Lichter A, Eshel D (2016) The role of aquaporins in ph-dependent germination of Rhizopus delemar spores. PLoS One **11**: 1–18

Tyerman SD, Niemietz CM, Bramley H (2002) Plant aquaporins: Multifunctional water and solute channels with expanding roles. Plant, Cell Environ **25**: 173–194

Wallach R, Da-Costa N, Raviv M, Moshelion M (2010) Development of synchronized, autonomous, and self-regulated oscillations in transpiration rate of a whole tomato plant under water stress. J Exp Bot **61**: 3439–3449

Wang Y, Liu F, Jensen CR (2012) Comparative effects of deficit irrigation and alternate partial root-zone irrigation on xylem pH, ABA and ionic concentrations in tomatoes. J Exp Bot **63**: 1907–1917

Wang Y, Noguchi K, Ono N, Inoue S, Terashima I, Kinoshita T (2014) Overexpression of plasma membrane H+-ATPase in guard cells promotes light-induced stomatal opening and enhances plant growth. Proc Natl Acad Sci U S A **111**: 533–8

Wigoda N, Pasmanik-Chor M, Yang T, Yu L, Moshelion M, Moran N (2017) Differential gene expression and transport functionality in the bundle sheath versus mesophyll – a potential role in leaf mineral homeostasis. J Exp Bot **68**: 3179–3190

Wilkinson S, Corlett JE, Oger L, Davies WJ (1998) Effects of xylem pH on transpiration from wild-type and flacca tomato leaves1. Plant Physiol **117**: 703–709

Wilkinson S, Davies WJ (1997) Xylem sap pH increase: A drought signal received at the apoplastic face of the guard cell that involves the suppression of saturable abscisic acid uptake by the epidermal symplast. Plant Physiol **113**: 559–573

Wu F, Shen S, Lee L, Lee S, Chan T, Lin C (2009) Tape-Arabidopsis Sandwich - a simpler Arabidopsis protoplast isolation method. Plant Methods **10**: 1–10

Wysocka-Diller JW, Helariutta Y, Fukaki H, Malamy JE, Benfey PN (2000) Molecular analysis of SCARECROW function reveals a radial patterning mechanism common to root and shoot. Development **127**: 595–603

Yamauchi S, Takemiya A, Sakamoto T, Kurata T, Tsutsumi T, Kinoshita T, Shimazaki K (2016) Plasma membrane H+-ATPase1 (AHA1) plays a major role in Arabidopsis thaliana for stomatal opening in response to blue light.

Plant Physiol **171**: pp.01581.2016

Yaneff A, Sigaut L, Gómez N, Aliaga Fandiño C, Alleva K, Pietrasanta LI, Amodeo G (2016) Loop B serine of a plasma membrane aquaporin type PIP2 but not PIP1 plays a key role in pH sensing. Biochim Biophys Acta - Biomembr **1858**: 2778–2787

Zhang X, Wang H, Takemiya A, Song C, Kinoshita T, Shimazaki K (2004) Inhibition of blue light-dependent H 1 Pumping by abscisic acid through hydrogen peroxide-induced dephosphorylation of the plasma membrane. Plant Physiol **136**: 4150–4158

Zimmermann MH (1983) Xylem Structure and the Ascent of Sap. doi: 10.1007/978-3-662-22627-8

Main Figure Legends

FIGURE 1. Leaf xylem sap pH reduced by petiole-fed fusicoccin (an AHA stimulator), and increased by vanadate (an AHA inhibitor) in minor veins in detached leaves of WT (wild type) Arabidopsis. **A.** Representative images of treatment effects with color-coded pH values calculated ratiometrically for all pixels which passed the selection criteria (Supplementary Materials and methods), with black masking all other pixels. i, low-K^+ control (i.e., XPS, xylem perfusion solution). ii, XPS + fusicoccin (10 µM). iii, high-K^+ control solution (XPS +10 mM KNO_3). iv, XPS +10 mM KNO_3 + vanadate (1 mM Na_3VO_4). **B.** The mean (±SE) xylem sap pH without and with fusicoccin in the indicated number of leaves (biological repeats) from at least three independent experiments. Asterisks denote significant differences from the respective control, using Student's two-tailed unpaired t-test (*: $P < 0.05$, **:

P < 0.001). Where error bar is invisible, SE= 0.009. Other details as in A. **C.** The mean (±SE) calculated values of the xylem sap pH without and with vanadate. Other details as in B.

FIGURE 2. Knockout of *AHA2* increases xylem sap pH in minor leaf veins of Arabidopsis leaf. *aha2* knockout lines and WT plants. The mean (±SE) xylem sap pH in the indicated number of leaves, from three independent experiments. Different letters denote significantly different pH values (P< 0.05; ANOVA).

FIGURE 3. Expression levels of *AHA2* and *AHA1* and xylem sap pH in leaves of WT, *aha2-4*, and in two independent bundle-sheath-specific AHA2-complimented lines (T55, T56). **A.** Mean normalized (±SE) *AHA2* expression levels obtained by qRT-PCR on whole leaf RNA (n=5 biological repetitions, leaves; see Suppl. Materials and methods). **B.** Mean (±SE) xylem sap pH in the indicated number of leaves from three independent experiments. Different letters indicate significantly different means (*P*<.0.05; ANOVA). **C.** Mean normalized (±SE) *AHA1* expression levels; other details as in A.

FIGURE 4. FIGURE 4. The leaf hydraulic conductance (Kleaf) depends on the activity of AHA2 and the pH of the xylem perfusion solution (XPS). Mean (±SE) Kleaf (calculated by Eq. 1, Materials and Methods) in detached Arabidopsis leaves. A. Leaves of WT and AHA2 mutant (aha2-4, aha2-5) plants perfused with non-buffered XPS. Numbers are those of assayed leaves (in three independent experiments). Different letters indicate significantly different means (P<.0.05; ANOVA). B. Leaves of WT, aha2-4 and SCR:AHA2 plants perfused with non-buffered XPS. The experiments in A and B were done at different time regimes and with different solutions (see Materials and Methods). The numbers and letters are as in A. Note that only

the aha2 Kleaf is lower relative to WT. C. WT Arabidopsis leaves fed with buffered XPS (XPSb) with the indicated pH. The numbers and letters are as in A. Note the lower Kleaf at the alkaline pH.

Figure 5: The effect of pH treatment on the membrane osmotic water permeability coefficient (P_f) of BSCs from SCR:GFP plants. A. Time course (60 sec) of bundle sheath protoplasts swelling upon exposure to a hypotonic XPS^{db} solution at pH 6 or 7.5. The arrow indicates onset of bath flush. B. Time course of the osmotic concentration change in the bath (Cout) during the hypotonic challenge (calculated as in Moshelion et al., 2004). C. Mean (±SE) initial P_f values of the indicated number of bundle sheath protoplasts under the different pHs from three independent experiments. The asterisk denotes a significant difference between the treatments using Student's two-tailed unpaired t-test ($P < 0.01$).

Fig 6. K_{leaf} as a function of intra-xylem "natural" pH. The pH of unbuffered XPS was modified naturally in detached leaves as a result of AHA2 mutation and its complementation (data combined from figures 3B and 4B). From left to right: SCR:AHA2, WT, aha2-4. Dashed lines: hand drawn to aid in trend visualization. Different letters denote significantly different means (a, b, ab – Kleaf values, c-e – pH values). Note the inverse relationship between K_{leaf} and XPS pH at the range pH 6-7.5).

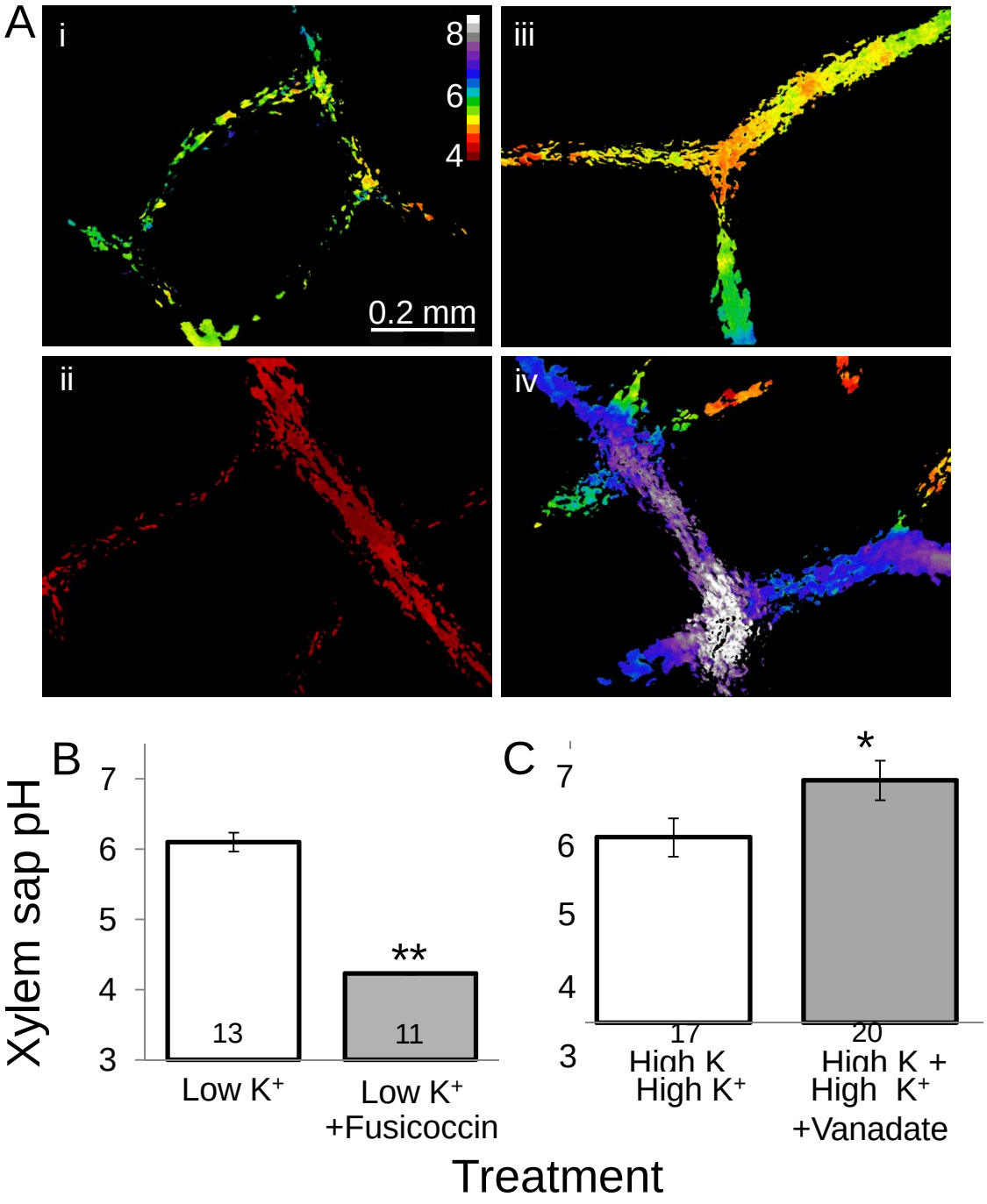

FIGURE 1. Leaf xylem sap pH reduced by petiole-fed fusicoccin (an AHA stimulator), and increased by vanadate (an AHA inhibitor) in minor veins in detached leaves of WT (wild type) Arabidopsis. **A.** Representative images of treatment effects with color-coded pH values calculated ratiometrically for all pixels which passed the selection criteria (Supplementary Materials and methods), with black masking all other pixels. i, low-K^+ control (i.e., XPS, xylem perfusion solution). ii, XPS + fusicoccin (10 μM). iii, high-K^+ control solution (XPS +10 mM KNO_3). iv, XPS +10 mM KNO_3 + vanadate (1 mM Na_3VO_4). **B.** The mean (±SE) xylem sap pH without and with fusicoccin in the indicated number of leaves (biological repeats) from at least three independent experiments. Asterisks denote significant differences from the respective control, using Student's two-tailed unpaired t-test (*: $P < 0.05$, **: $P < 0.001$). Where error bar is invisible, SE= 0.009. Other details as in A. **C.** The mean (±SE) calculated values of the xylem sap pH without and with vanadate. Other details as in B.

Fig. 1. Grunwald, Wigoda et al, 2019

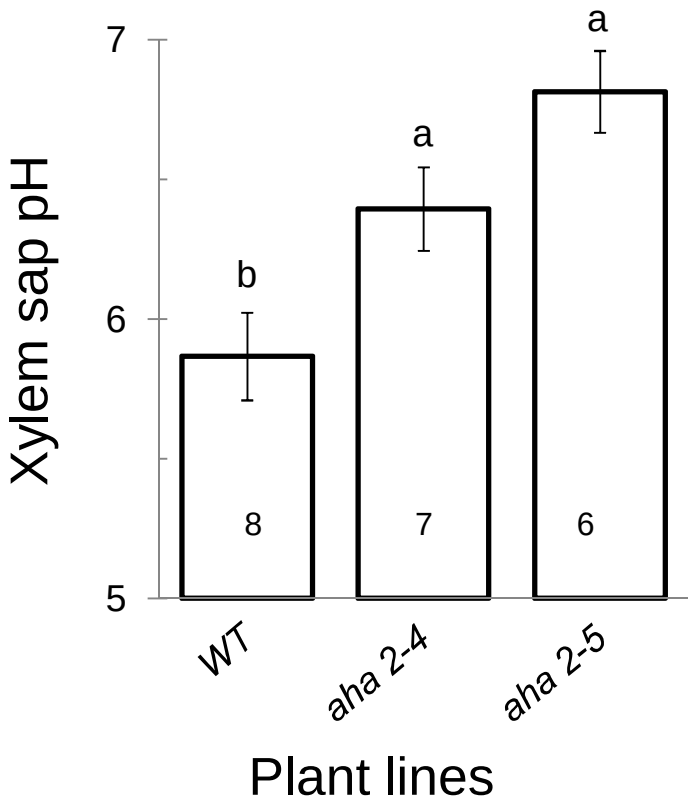

FIGURE 2. Knockout of *AHA2* increases xylem sap pH in minor leaf veins of Arabidopsis leaf. *aha2* knockout lines and WT plants. The mean (±SE) xylem sap pH in the indicated number of leaves, from three independent experiments. Different letters denote significantly different pH values ($P < 0.05$; ANOVA).

Fig. 2. Grunwald, Wigoda et al, 2019

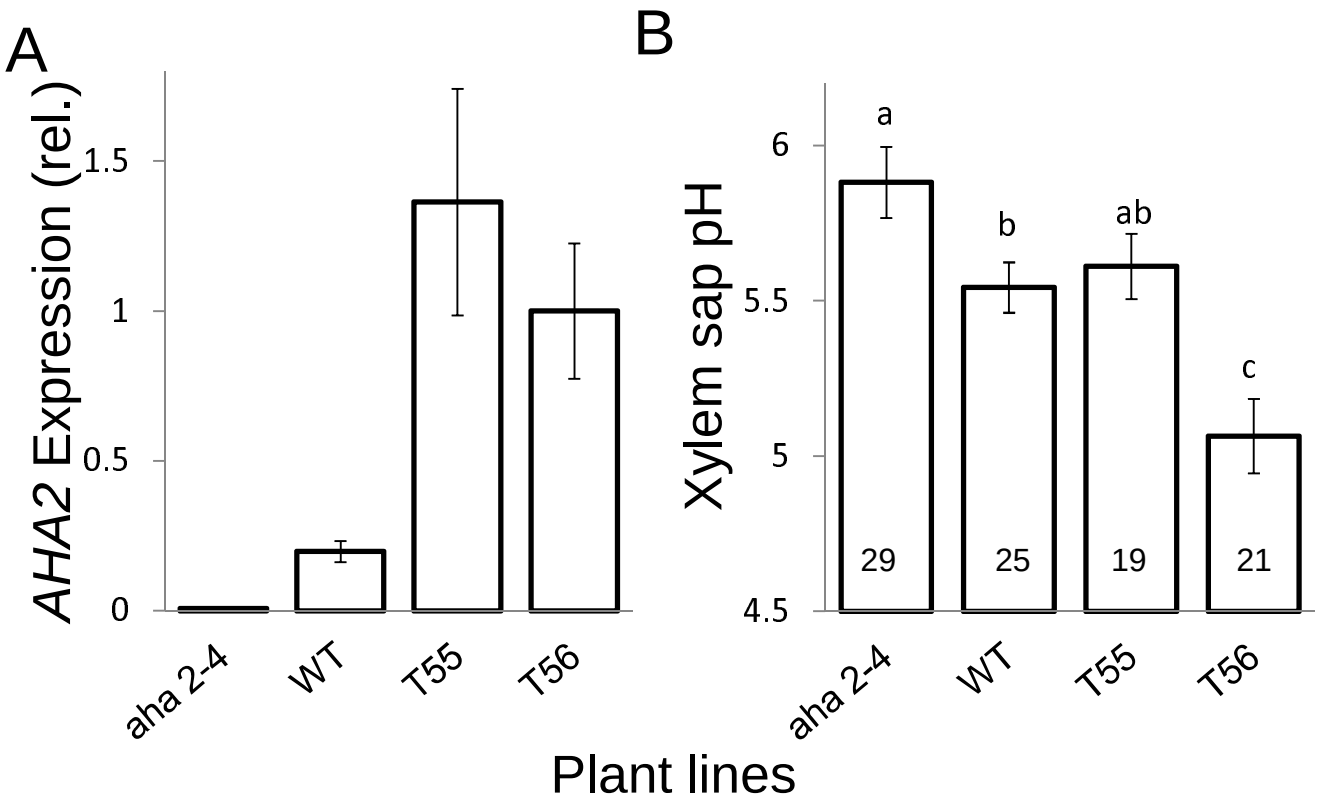

FIGURE 3. Expression levels of *AHA2* and xylem sap pH in leaves of WT, *aha2-4* and of two independent lines (T55, T56) of aha2-4 complemented with AHA2 under a bundle-sheath-specific promotor (SCR:AHA2). A. Mean normalized (±SE) *AHA2* expression levels obtained by qRT-PCR on whole leaf RNA (n=5 biological repetitions, leaves; **B.** Mean (±SE) xylem sap pH in the indicated number of leaves from three independent experiments. Different letters indicate significantly different means ($P<.0.05$; ANOVA).

Fig. 3. Grunwald, Wigoda et al, 2019

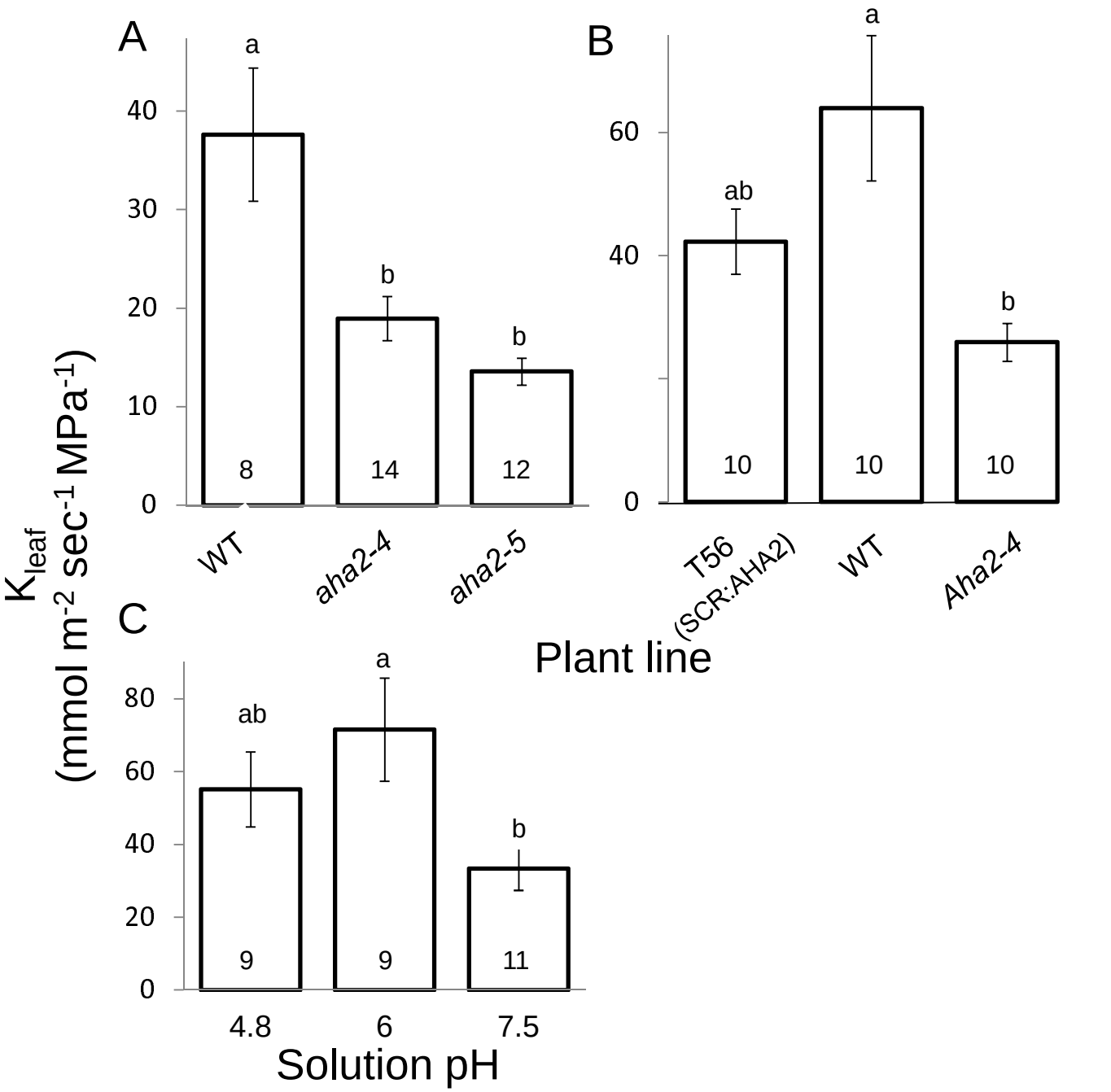

FIGURE 4. The leaf hydraulic conductance (K_{leaf}) depends on the activity of AHA2 and the pH of the xylem perfusion solution (XPS). Mean (±SE) K_{leaf} (calculated by Eq. 1, Materials and Methods) in detached Arabidopsis leaves. **A.** Leaves of WT and *AHA2* mutant (*aha2-4*, *aha2-5*) plants perfused with non-buffered XPS. Numbers are those of assayed leaves (in three independent experiments). Different letters indicate significantly different means (P<.0.05; ANOVA). **B.** Leaves of WT, *aha2-4* and *SCR:AHA2* (T56) plants perfused with non-buffered AXS. (see Materials and Methods). The numbers and letters are as in A. **C.** WT Arabidopsis leaves fed with XPS^{db} buffered to the indicated pH. The numbers and letters are as in A. Note the lower K_{leaf} at the alkaline pH.

Fig. 4. Grunwald, Wigoda et al, 2019

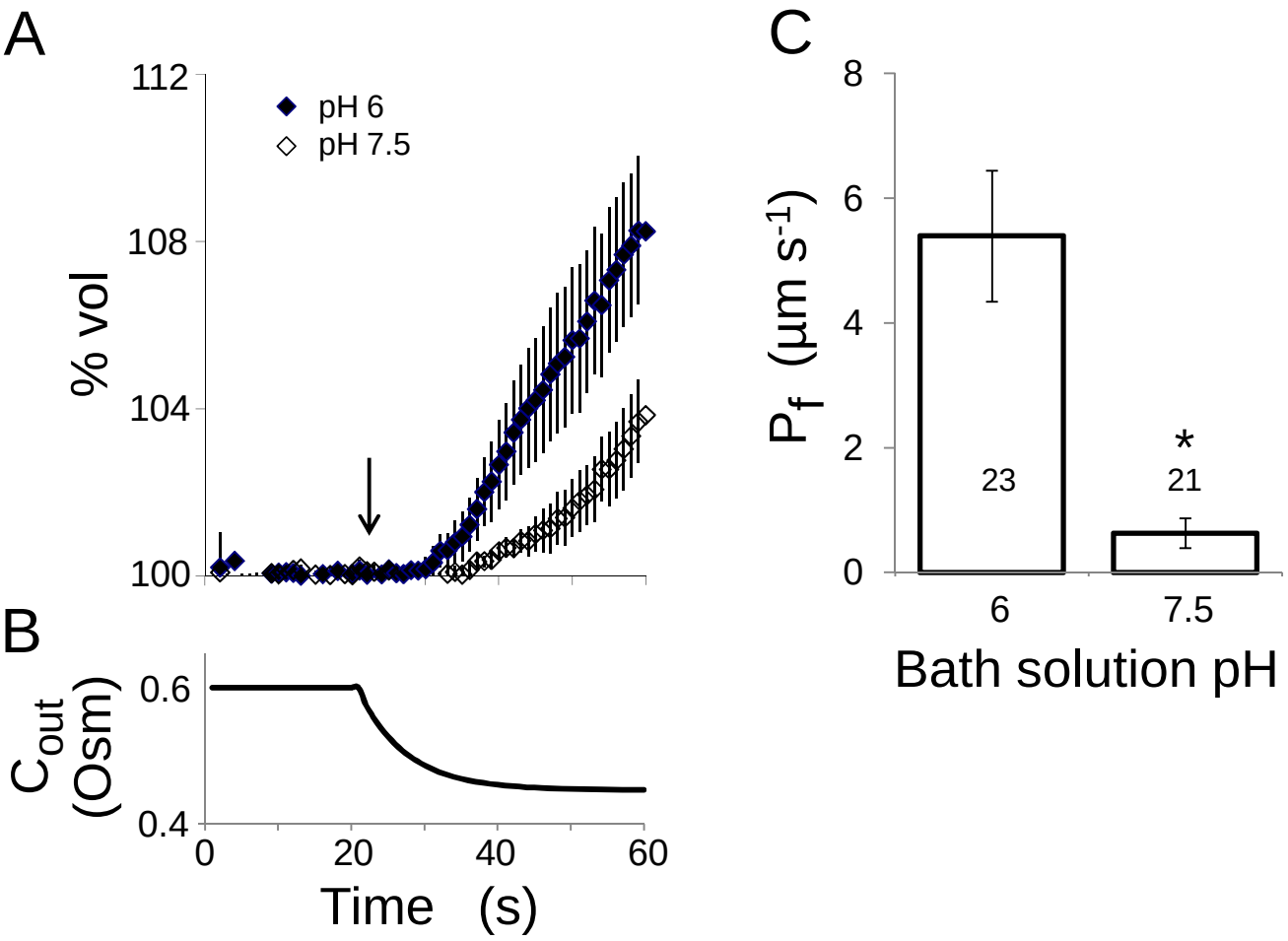

Figure 5: The effect of pH treatment on the membrane osmotic water permeability coefficient (P_f) of BSCs from SCR:GFP plants. **A.** Time course (60 sec) of bundle sheath protoplasts swelling upon exposure to a hypotonic XPS^{db} solution at pH 6 or 7.5. The arrow indicates onset of bath flush. **B.** Time course of the osmotic concentration change in the bath (Cout) during the hypotonic challenge (calculated as in Moshelion et al., 2004) . **C.** Mean (±SE) initial P_f values of the indicated number of bundle sheath protoplasts under the different pHs from three independent experiments. The asterisk denotes a significant difference between the treatments using Student's two-tailed unpaired t-test ($P < 0.01$).

Fig. 5. Grunwald, Wigoda et al, 2019

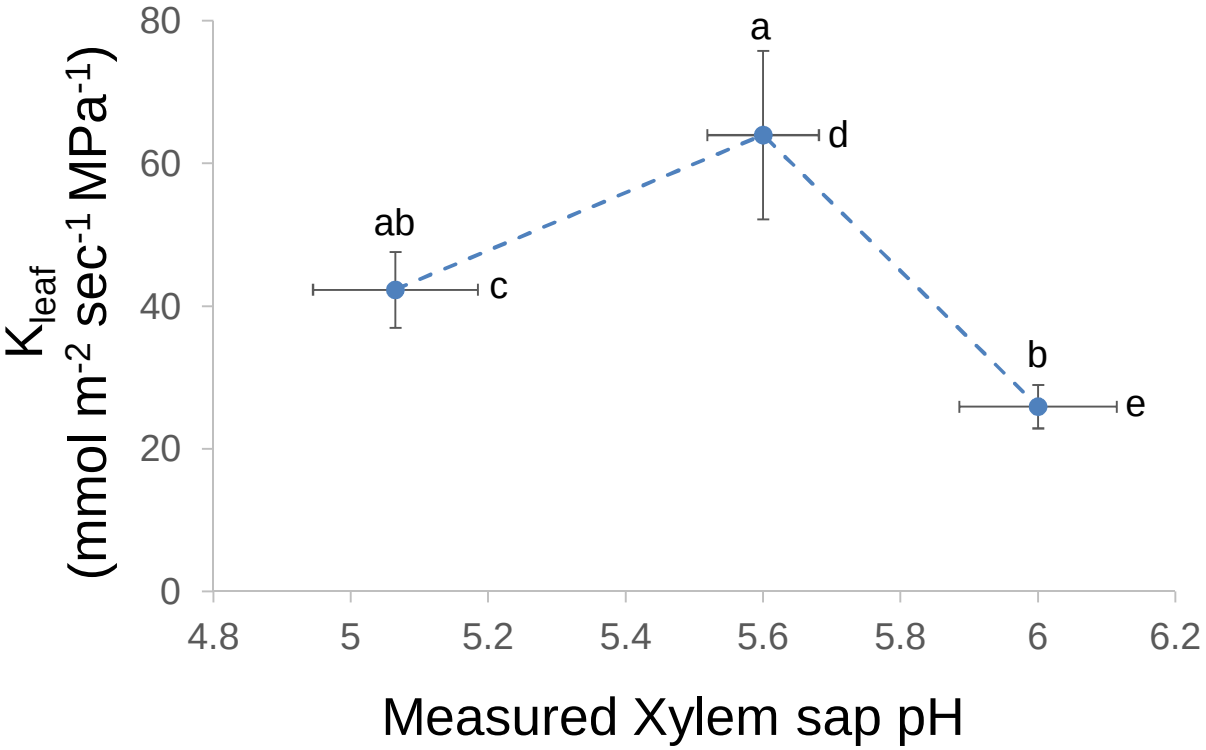

FIGURE 6. **K_{leaf} as a function of intra-xylem pH**. The detached leaves modified the pH of the unbuffered XPS within their xylem depending on AHA2 presence. Combined data from figures 3B (here: on the abscissa) and 4B (here: on the ordinate). From left to right: SCR:AHA2 (T56), WT, aha2-4. Dashed lines: hand drawn to aid in trend visualization. Different letters denote significantly different means (a, b, ab: K_{leaf} values, c-e: pH values). Note the inverse relationship between K_{leaf} and XPS pH at the pH range 5.6-6).

Fig. 6. Grunwald, Wigoda et al, 2019